PERFORMANCE ASSESSMENT OF THE NUCLEAR CYCLER CONCEPT Nicolas Thiry[1], C. Tardioli [1], M. Vasile[2], University of Strathclyde, Glasgow, G1 1XJ united Kingdom; nicolas.thiry@strath.ac.uk

Keywords: *Asteroid deflection, planetary defence, nuclear interceptor*

Abstract: The nuclear cycler is a variant of the stand-off nuclear blast technique for asteroid deflection. The main idea behind the nuclear cycler is to go from a single shot deflection strategy to an incremental one in which multiple nuclear bombs can be deployed from a vantage point at a distance from the asteroid. The spacecraft carrying the bombs is maintained in formation with the asteroid, exploiting natural dynamics, and periodically drops a bomb probe that detonates at the optimal altitude from the target. It can be demonstrated that this incremental approach provides performance comparable to a single explosion but with a higher degree of controllability and redundancy. The model presented in this paper takes into account the shape and composition of the asteroid. A number of these key physical parameters, such as total vaporization enthalpy or the detonation altitude are affected by a degree of uncertainty that can significantly affect the outcome of a deflection. The paper will present a preliminary uncertainty analysis and a robust deflection strategy that accounts for uncertainty in the key model parameters. The uncertainty region in the model parameter space is propagated together with the uncertainty in the initial conditions to derive the dispersion of all the possible virtual impactors on the impact plane at the Earth. The control of the deflection action is then optimised to minimise the collision risk.

Introduction:

Deflection methods are commonly divided into two main categories, impulsive and slow push, depending on whether the modification of the orbit of the asteroid is, respectively, quasi-instantaneous or needs to be acted over a longer period of time. Examples of impulsive methods include the nuclear interceptor [12] and the kinetic impactor [2] while slow-push methods include, among others, the gravity tractor [3], the laser ablation [14], the ion-beam shepherd [4] and the mass driver [5]. The nuclear interceptor would allow nudging the asteroid out of its collision course with the Earth even when the warning time is low but a single explosion represents a single point of failure and does not allow controlling the evolution of the trajectory of the asteroid. On the other hand, slow-push methods allow for a more precise control of the deflection manoeuvre but typically require a longer warning time, additional propellant in order to maintain a hovering position in the vicinity of the asteroid, the ability to operate autonomously and are dependent on their distance from the Sun[4, 8, 14]. Nuclear methods carry the highest energy density among all the other mitigation strategies. Since there is no atmosphere in space, the efficiency of nuclear methods is based on the amount of asteroid material that can be blasted away following the explosion. In a 2007 report to Congress, [10] argued that using a stand-off nuclear detonation would be ten to a hundred times more effective than any other alternative. While a subterranean explosion would in principle further increase the amount of material that can be expelled, a stand-off configuration does not require landing and digging and is thus more manageable with current technology.

The theoretical efficiency of nuclear-based approaches must be balanced with the difficulty in controlling the outcome of the explosion. This lack of control can lead to three main problems. The high level of energy released during the single detonation introduces the potential risk of an unwanted fragmentation. If the asteroid breaks up into several pieces following the explosion, it may be that some of the larger pieces still impact the Earth and the probability of causing damages may never go to zero [6] (note however that the risk of fragmentation is already reduced due to the choice of the stand-off configuration). Another problem arise from the precise detonation at the required location. Choosing such a location could actually require the addition of an observer spacecraft, as it is the case for the kinetic impactor. Last but not least, the current epistemic uncertainty on the properties of the asteroid translates into a significant variance on the expected deflection. In particular, as it will be shown in this paper, the efficiency of the nuclear interceptor relies strongly on the amount of energy required to vaporize the asteroid material which itself is not so well characterized in the available literature. Hence, relying on a single interceptor could be a rather risky strategy.

The idea proposed in this paper is to partially overcome these difficulties by fractionating a single explosion into a number of smaller and better controlled ones. A single spacecraft, carrying a number of bombs, is placed on a formation orbit with the asteroid and incrementally releases the bombs so that each of them explodes at an optimal position with respect to the surface of the asteroid. As it will be shown, a careful choices of the firing time and orbital trajectory can allow for incrementally deflecting the asteroid while ensuring an appropriate radiation shielding to the carrier.

The paper is structured as follows: we start by reviewing the model of a single nuclear interceptor method considering a spherical and an elongated asteroid. We then explain the idea of the nuclear cycler and illustrate the concept with a possible choice of mission config-

uration. We then perform a result comparison for the deflection of an elongated Apophis-like asteroid using a single interceptor and an incremental deflection using the nuclear cycler idea. The paper also addresses the impact on performances due to the degree of uncertainty on two key parameters of the problem: the distance of detonation and the total vaporization enthalpy. We follow these by a discussion and finally conclude on the strategy and give plans for future works.

Single Detonator Model:

This section introduces a simple model to calculate the change in linear momentum of the asteroid due to a stand-off nuclear explosion, and consists in a slightly modified version of the model presented by [8] applicable to the case of a spherical asteroid. Our model is also extended to the case of an elongated body with ellipsoidal shape.

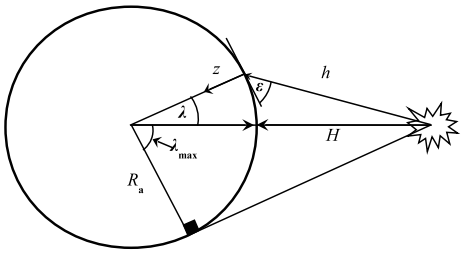

Figure 1: Standoff configuration for the nuclear interceptor method

The energy released during the explosion is carried by the debris of the exploded spacecraft and by the radiations. Table 1 shows the fraction f_i (with $i \in \{1, 2, 3, 4, 5\}$) of energy associated to each of the products of the explosion for the case of a fusion and fission devices [11, 12]. The energy delivered during

Source	1-X-ray	2-Neutrons	3-Gamma rays	4-Debris	5-Others
Fission	0.7	0.01	0.02	0.2	0.07
Fusion	0.55	0.2	0.01	0.2	0.04

Table 1: Energy fraction f_i over all the products of a nuclear explosion

the explosion, Y_0, is computed from the yield-to-mass ratio and is conservatively assumed to have a value YTW=0.75 ktons/kg for fusion devices and $YTW = 0.075$ ktons/kg for fission devices [1]:

$$Y_0 = YTW m_{wh} \tag{1}$$

where m_{wh} is the mass of the bomb. In this paper, no buried or surface detonation are considered due to the added difficulty of landing and digging on an asteroid and only stand-off explosions are modelled.

With reference to Fig.1, the explosion is assumed to happen at a distance H from the surface of the asteroid, therefore, only a portion m_{debris} of the total mass of debris m_d will hit the surface:

$$m_{debris} = S m_d \tag{2}$$

If one assumes that the exploding device sees a spherical cap with radius R_A, then the fraction S can be expressed as:

$$S = \frac{1}{2} - \frac{\sqrt{H}}{2}\frac{\sqrt{H + 2R_A}}{R_A + H} \tag{3}$$

The ejection velocity of the debris v_{debris} is then computed from the fraction $f_4 = 0.2$ (see Table1) of the total energy Y_0 released during the blast:

$$v_{debris} = \sqrt{\frac{2 f_4 Y_0}{m_d}} \tag{4}$$

The variation of velocity δv_{debris} due to the debris cloud only is then given by:

$$\delta v_{debris} = \beta S_{sc} \frac{m_{debris} v_{debris}}{m_A} \tag{5}$$

where S_{sc} is a scattering factor and β the momentum enhancement factor [9] which is conservatively assumed to a value of 2.

The contribution from the radiations is derived from the Beer-Lambert law of absorption. Given a radiation with frequency ν and knowing the incident radiation energy per unit area $I_0^\nu(\lambda)$ and the depth z, the energy per unit area $I^\nu(\lambda, z)$ transmitted beyond a given depth is computed as follows:

$$I^\nu(\lambda, z) = \sin\epsilon(\lambda) I_0^\nu(\lambda) \exp\left(-\rho_A \kappa_\nu \frac{z}{\sin\epsilon(\lambda)}\right) \tag{6}$$

The incident radiation density $I_0^\nu(\lambda)$ is given by:

$$I_0^\nu(\lambda) = \frac{f_i}{4\pi h^2(\lambda)} Y_0 \tag{7}$$

where the h distance is computed as:

$$h = \sqrt{(H + (1 - \cos\lambda) R_A)^2 + R_A^2 \sin^2\lambda} \tag{8}$$

and ϵ is given by:

$$\sin\epsilon = \frac{(R_A + H)\cos\lambda - R_A}{h} \tag{9}$$

The linear mass-absorption coefficient κ_ν for each type of radiation is given in Table 2 [12]. Note that

[1] From data available online at http://nuclearweaponarchive.org/

Radiation type	X-Ray	Neutron	Gamma ray
Value	1.5 m^2/kg	0.0044 m^2/kg	0.005 m^2/kg

Table 2: Opacity κ_ν, or linear mass-absorption coefficient, for an asteroid made of forsterite

quantities in Table 2 are to be considered as mean values over the range of frequencies of X-rays and Gamma-rays.

The amount of energy absorbed per unit mass at a given depth is then obtained by considering the cumulative absorption of each radiation type:

$$E(\lambda, z) = -\sum_\nu \frac{dI^\nu}{dz} = \sum_\nu \kappa_\nu I_0^\nu \exp\left(-\rho_A \kappa_\nu \frac{z}{\sin\epsilon(\lambda)}\right) \tag{10}$$

Part of this energy goes into the vaporization process of the asteroid, while the excess energy is converted into thermal excitation. The local average velocity of the gas molecules can then be estimated by writing a simple energy balance with E_v the total vaporization enthalpy per unit mass:

$$\bar{v}(\lambda, z) = \sqrt{2(E(\lambda, z) - E_v)} \tag{11}$$

This allows one to define a limit depth z_{MAX} below which the vaporization process cannot continue as the energy absorbed is lower than the vaporization enthalpy. Given a certain distance H and yield Y_0, the value of z_{MAX} is numerically computed by finding the value of z that satisfies the relationship $E(\lambda, z) = E_v$ for each λ considered. The change in linear momentum generated by the expelled material is then expressed, for an infinitesimal volume, as:

$$dP = \frac{\cos\lambda}{2} \rho_A \bar{v}(\lambda, z) dV \tag{12}$$

where the cosine function comes from the fact that we only retain the tangential component and the $\frac{1}{2}$ factor is coming from the assumption of an equiprobable scattering of the gas molecules from the ablated surface over a hemisphere. The area of a spherical cap is given by:

$$S = 2\pi R_A^2 (1 - \cos\lambda) \tag{13}$$

The infinitesimal volume dV is thus given by:

$$dV = 2\pi R_A^2 \sin\lambda dz d\lambda \tag{14}$$

Integrating relation (12) and dividing by the mass of the asteroid eventually allows one to express the change of velocity $\delta v_{radiations}$ due to the radiations:

$$\delta v_{radiations} = \frac{\pi R_A^2}{M_A} \int_0^{\lambda_{MAX}} \int_0^{z_{MAX}(\lambda)} \rho_A \bar{v}(\lambda, z) dz \sin\lambda\cos\lambda d\lambda \tag{15}$$

Figure 2a shows the total $\delta v = \delta v_{radiations} + \delta v_{debris}$ imparted to an asteroid, with mass and density reported in Table 3, assuming a fusion device of 600kgs at different altitudes of detonation and for different values of the enthalpy of vaporization, while Figure 2b shows the δv imparted to the same asteroid by a fission device of equal mass at different altitudes of detonation and for different values of the enthalpy of vaporization.

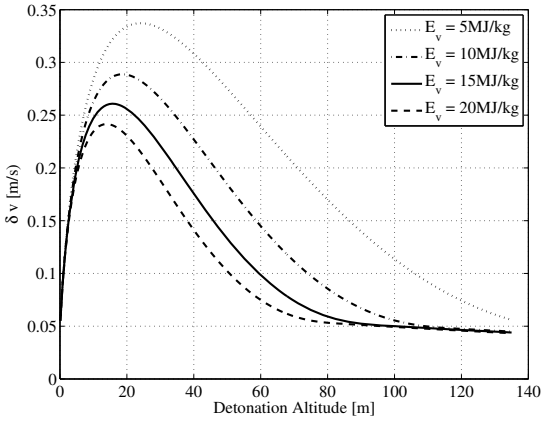

(a) 600kgs fusion device

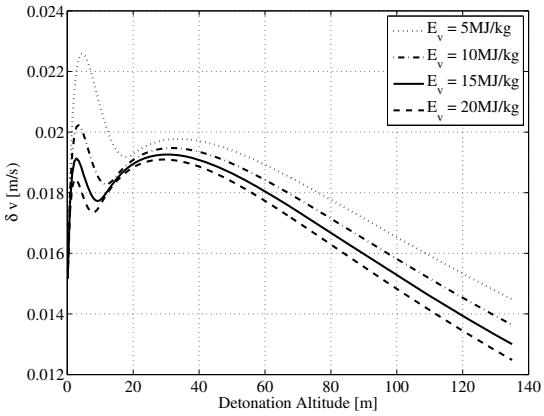

(b) 600kgs fission device

Figure 2: Impulsive change of velocity as a function of the detonation altitude for different values of the enthalpy of vaporization

the model can easily be extended to the case of an elongated asteroid with an elongation factor e_l - that is an ellipsoidal shape with semi-major axis $a_I = e_l^{2/3} R_A$ and semi-minor axes $b_I = c_I = \frac{R_A}{e^{1/3}}$. The mean radius is still identical to the one used in the spherical case previously derived, so that the elongated and the spherical asteroids considered have an identical volume. Considering as a worst case scenario the configuration where the bomb is detonated along the longer side, the distance

$h(\lambda)$ is now given as

$$h = \sqrt{(H + (1 - \cos\lambda)e_l^{2/3}R_A)^2 + \left(\frac{R_A}{e_l^{1/3}}\right)^2 \sin^2\lambda} \tag{16}$$

We need now to distinguish between λ, the angle in elliptical coordinates corresponding to the concentric circle or radius a_I and $\tilde{\lambda}$, the angle between the normal to the ellipsoidal surface and the horizontal direction. They can be related through the following formula:

$$\cos\tilde{\lambda} = \frac{\cos\lambda}{\sqrt{1 + (e_l^2 - 1)\sin^2\lambda}} \tag{17}$$

The value of $\sin\epsilon$ is obtained by computing the scalar product between the direction normal to the ellipsoidal surface $\mathbf{n}$ and the direction $-\mathbf{h}$, which gives

$$\sin\epsilon = \frac{\frac{e_l^{2/3}R_A + H}{e_l^{2/3}R_A}\cos\lambda - 1}{\frac{e_l^{1/3}h}{R_A}\sqrt{\frac{\cos^2\lambda}{e_l^2} + \sin^2\lambda}} \tag{18}$$

Last but not least, the infinitesimal volume is now expressed as

$$dV = 2\pi e_l^{1/3}R_A^2\frac{\sin^2\lambda}{\sin\tilde{\lambda}}dzd\lambda \tag{19}$$

Keeping a constant detonation altitude of 17m, Fig. 3 shows how the δv produced compares to the spherical case, considering again a 600 kgs fusion device.

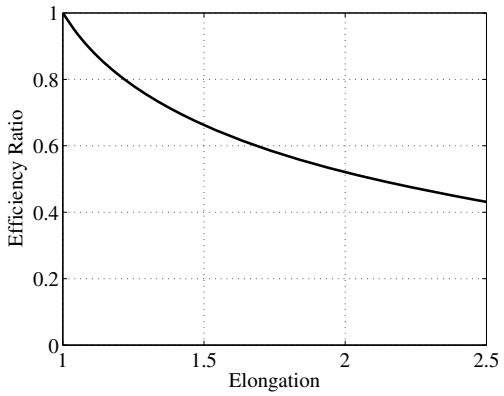

Figure 3: Performance comparison between the spherical case and a cigar-shaped asteroid as a function of the elongation

Nuclear Cycler Mission Concept and Design:

The key idea is to incrementally change the velocity of the asteroid by releasing and detonating a series of relatively small nuclear bombs from a vantage point at a safety distance from the asteroid. Fig. 4 shows a possible configuration with a carrier-spacecraft flying in formation with the asteroid on a periodic orbit at a distance from the asteroid and releasing two bombs at two different times. The detonation occurs on the far side of the asteroid, with respect to the spacecraft so that the asteroid is shielding the spacecraft from radiations and debris. In this particular configuration, the orbit of the carrier and the one of the bomb are timed in such a way that by the time the bomb goes from point A to point C, the carrier has moved from point A to point B and by the time the bomb goes from B to C, the carrier has moved from B back to A, closing the cycle. A new cycle can now begin. In addition, the data from the previous explosions can be collected and analysed to control the altitude and timing of the subsequent explosions or to control the direction of the resulting $\delta\mathbf{v}$. In the remainder of this paper we will analyse only the special configuration in which point A corresponds to the perihelion of the orbit of the asteroid and point B the aphelion. In this case two bombs are released every revolution of the asteroid around the Sun.

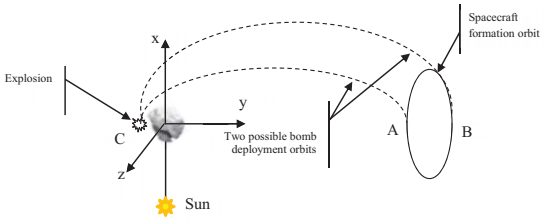

Figure 4: Sketch (not to scale) of the nuclear cycler concept.

Comparison Between a Single Detonator and the Nuclear Cycler:

The nuclear cycler method has been applied to the case of an Apophis-like asteroid considering a warning time of 3 years. The warning time is here defined as the time from the first explosion to the expected impact of the un-deviated asteroid with the Earth. Relevant properties of this asteroid can be found in Table 3. The initial inclination, right ascension, argument of the pericentre and mean anomaly were set so that the asteroid impacts the Earth on 13140 MJD.

An interesting first result is obtained by computing the total δv produced by either a single or a fractionated detonation for the same total mass of the bombs. The results of our model, in Fig. 5, indicate that a fractionated explosion may be better than a single explosion for the same total mass. The explanation of this result is in the dependency of the δv on the view angle λ in Eq. (15) and the penetration depth z_{MAX}. Figure 6 shows the optimal detonation altitude as a function of the space-

Element		Measured Value
Semi-major axis	a_0	0.9224 AU
Eccentricity	e_0	0.1912
Period	T_0	323.5969 days
Mean motion	n_0	1.2876 $\times 10^{-5}$ deg/s
Mass	m_A	2.7×10^{10} kg
Gravit. constant	μ_A	$1.801599 \times 10^{-9} km^3/s^2$
Phys. dimensions	a_I, b_I, c_I	196 m, 112 m, 112 m
Rot. velocity	w_A	3.3×10^{-3} deg/s
Tot. vap. Enthalpy	E_v	15MJ/kg
Density	ρ_A	2650 kgs/m^3

Table 3: Orbital and physical properties of test asteroid.

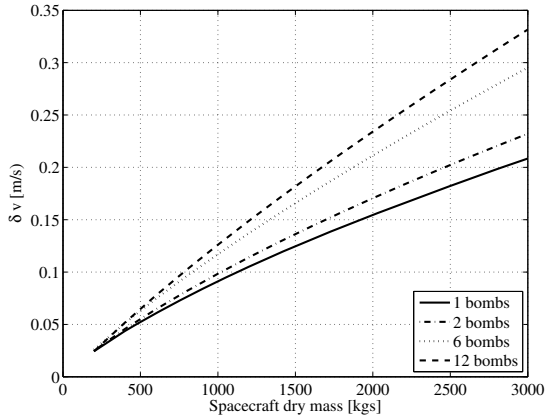

Figure 5: Total δv as a function of the dry mass of the spacecraft for different numbers of explosions

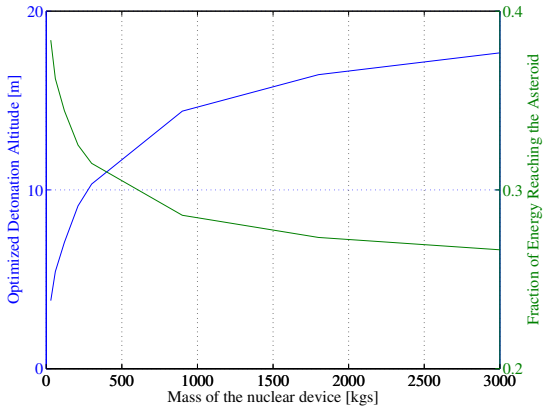

Figure 6: Optimal altitude of detonation and fraction of the total energy reaching the asteroid for different sizes of the nuclear device

craft mass for a single interceptor. One can see that the optimal altitude is indeed lower for a smaller bomb, therefore, the fraction of the total released energy actually reaching the asteroid is bigger in this case.

However, once the deflection parameter b (representing the projection of the deflection distance computed from on the target plane) is used as performance indicator, one can see, in Fig. 7, that the single interceptor method outperforms the cycler one, thanks to the fact that the whole velocity variation is delivered at the very beginning of the first cycle and thus its effect propagates for a longer period. The comparison is done by considering identical dry masses of the spacecraft with the cumulative mass of the nuclear bombs representing 30 % of the total dry mass of the spacecraft in both cases. For the single interceptor method, the whole mass of the spacecraft contributes to the ejecta, whereas only the mass of the bombs contributes to ejecta for the cycler method. Last but not least, in both cases, the detonation occurs at the optimal altitude. Also note that a warning time of only 3 years constrains the maximum number of explosion to 6 for the nuclear cycler method if explosions occur only at the apsidal points. Another interesting result is obtained by normalising the value of the b parameter obtained for the case of a fractionated detonation with the result of the single interceptor method. The results in Fig. 8 indicate that the mass efficiency (the ratio between b parameter and mass of the spacecraft) can be as low as 40% for small spacecraft and reduces to 75% for larger spacecraft.

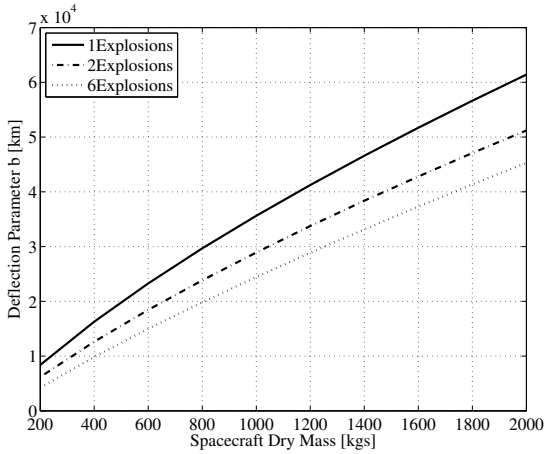

Figure 7: Deflection parameter for a varying number of explosions and a 3 years lead time

Uncertainty Propagation:

The model presented in this paper takes into account the shape and composition of the asteroid. A number of these key physical parameters such as the total vaporization enthalpy, the detonation altitude or the absorptivity are affected by a degree of uncertainty that can signifi-

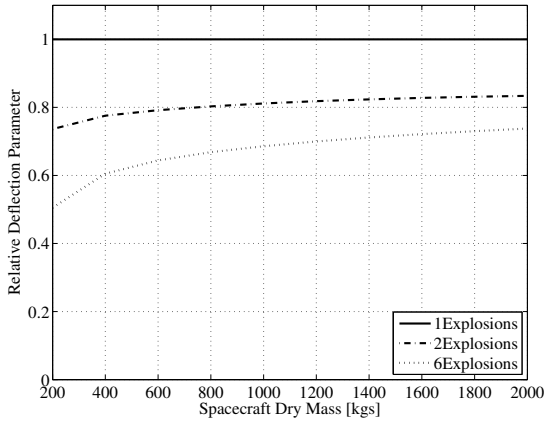

Figure 8: Efficiency of the nuclear cycler method compared to the single interceptor method for a 3 years lead time

cantly affect the outcome of a deflection. In this section we present a preliminary uncertainty analysis that accounts for uncertainty in the total vaporization enthalpy and the detonation altitude.

The uncertainty region in the model parameter space is propagated together with the uncertainty in the initial conditions to derive the dispersion of all the possible virtual impactors on the target plane centred in the Earth at the time of impact.

Each state variables has been approximated with a linear combination of multivariate Chebyshev polynomials. The unknown coefficients have been computed using a Lagrange interpolation. Since the number of coefficients grows as $\Delta_{d,n} = (d+n)!/(d!n!)$ with d the number of variables and n the degree of the polynomial expansion, the sampling points for the interpolation have been taken from a sparse grid instead of a tensor product. In particular we used the results of [18] to construct both the sparse grid with Chebyshev extrema and the Chebyshev polynomial basis.

The uncertain parameters are $\mathcal{E}_0 \in \mathbb{R}^6$, the state vector, and $H^{(j)}, E_v^{(j)} \in \mathbb{R}$, the altitude and the total vaporization enthalpy, respectively, at each detonation stage i, for $i = 1, \ldots, n_{expl}$, where n_{expl} is the number of explosions. For example, for $n_{expl} = 6$ and a level of the grid equal to 2, we have $d = 24$ uncertain parameters and $1,201$ sample points in a Smoliack sparse grid.

The number of sampling points at each stage can be kept constant by decomposing the polynomial approximations into n_{expl} parts. After each explosion, the uncertainty region is mapped in the hypercube $[-1,1]^d$, that is the domain of definition of a d-variate Chebyshev polynomial. This transformation can be easily obtained using the Principal Component Analysis (PCA).

	a[km]	h	k	p	q	L
Mean ($\mathcal{E}_0$)	$1.38e8$	0	0.01912	0	0	0
RMS (σ)	1.496	$4e^{-5}$	$5e^{-5}$	$6e^{-5}$	$5e^{-5}$	$5e^{-7}$

Table 4: Uncertainty region at initial epoch for the 6 Equinoctial orbital elements.

Therefore, after each explosion i we compute the approximation of $\mathcal{E}^{(i)}$ as a map of $\mathcal{E}^{(i-1)}, a^{(i-1)}, E_v^{(i-1)}$, only $d = 8$ uncertain parameters.

The polynomial approximation does not need any assumption on the probability distribution functions, therefore the initial uncertainty space for the state variable, represented by the 6 Equinoctial orbital elements [19], have been taken from the hypercube $[\bar{\mathcal{E}}_0 - 5\sigma_0, \bar{\mathcal{E}}_0 + 5\sigma_0]$, see Table 4. Whereas the altitude of detonation and the total vaporization enthalpy have been taken in the intervals $[0.1m\,, 40m]$ and $[10MJ/kg\,, 20MJ/kg]$, respectively.

Each uncertainty region has been model with a sparse grid of level 2, that corresponds to 145 sampling points and maximum degree of expansion 4.

To assess the probability of impact, we sample the uncertain variables assuming disjoint Gaussian distributions and propagate each point using the Chebyshev polynomial expansions. Figure 9 shows the projection of the uncertainty region on the target plane at collision time after 6 explosions. The probability distribution functions of the components of the b-parameter vector X_ξ and X_ζ is approximated with Gaussian distributions.

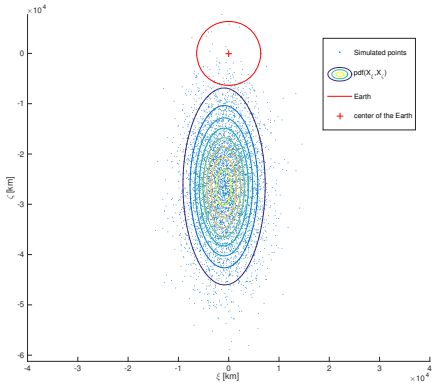

Figure 9: Projection of the uncertainty region on the target plane at impact after 6 explosions. The red circle is the Earth, while the ellipses represent the level curves of the probability distribution function of X_ξ and X_ζ up to 5σ.

Discussion: While discussing the results of the nuclear cycler method, it is important to keep in mind

the initial purpose of the method, which is to partially bridge the existent gap between impulsive methods and slow-push strategies. If one looks at the pure mass efficiency, the nuclear cycler was demonstrated to be less efficient than a single detonation, although for the cases investigated in this paper, our results indicate that the performance of the nuclear cycler method can remain relatively close to the the single interceptor's one. When the total mass allocated is the same, two opposite effects are responsible for an increase or a decrease in the performance. First, fractioning a large explosion in a sequence of smaller explosions seems beneficial in that the optimal detonation altitude is lower and thus the fraction of energy released during the explosion that impinges on the asteroid surface is higher. On the other hand, the effect of each explosion propagates for less time. This effect alone explains why, despite an augmented total δv, the performance of the cycler strategy is not as good as the single impulse method. On the other hand, the nuclear cycler offers a higher degree of redundancy and controllability that, in our opinion, largely outweighs the performance loss if sufficient warning time is available. Compared to slow push methods, the nuclear cycler still maintains the edge, due to higher energy density, although it requires similar navigation and control capabilities to maintain formation. It is however, not constrained to remain at close distance, does not suffer from contamination effects and is less sensitive to the distance from the Sun.

Conclusion and Future Works:

This paper proposed a novel deflection method, called nuclear cycler concept, derived from the nuclear interceptor concept. This incremental strategy bridges the gap between traditional impulsive and slow-push methods by combining the advantages of the single nuclear interceptor method, which is often quoted as the most effective way of deflecting an asteroid, with the superior controllability offered by slow push methods. The nuclear cycler approach could be used to precisely manipulate the trajectory of an asteroid with a high degree of redundancy, something not feasible by a single impulsive strategy. In addition, during a given cycle, the data generated by the past explosions can be investigated and fitted by the theoretical models in order to improve the efficiency of the next cycle. The analyses in this paper were limited to the case in which explosions occur at the apsidal points. More frequent explosions are possible but this analysis is left for future studies. Further analyses are also required in order to have a full picture regarding the range of applicability of the nuclear cycler method and to assess the impact of the different parameters the effectiveness of this method depends on.

Acknowledgement: This work is funded by the European Commission's Framework Programme 7, through the Stardust Marie Curie Initial Training Network, FP7-PEOPLE-2012-ITN, Grant Agreement 317185.

References: [1] Hammerling, P., Remo, J. L., NEO Interaction with Nuclear Radiation, Acta Astronautica, Vol. 36, No. 6, 337-346, 1995 [2] Jutzia, M., Michel, P. Hypervelocity impacts on asteroids and momentum transfer I. Numerical simulations using porous targets, Icarus Vol. 229, pp247-253, 2014 [3] Lu, E. T. 1, Love, S. G. Gravitational tractor for towing asteroids, Nature, Vol. 438, 177-178, 2005 [4] Bombardelli, C., Pelez, J., Ion Beam Shepherd for Asteroid Deflection, Journal of Guidance, Control and Dynamics, Vol. 34, No. 4, 2011 [5] Olds, J., Charania, A., Graham, M., Wallace, J., The League of Extraordinary Machines: A Rapid and Scalable Approach to Planetary Defense Against Asteroid Impactors, NASA Inst. for Advanced Concepts, CP-NIAC 02-02, Vol. 1, 2004 [6] Sanchez Cuartielles, J. P., Vasile, M., Radice, G. Consequences of asteroid fragmentation during impact hazard mitigation, Journal of Guidance, Control and Dynamics, 33, No. 1, 126-146, 2010 [7] Wie, B. Dynamics and Control of Gravity Tractor Spacecraft for Asteroid Deflection, Journal of Guidance, Control and Dynamics, 33, No. 5, 2008 [8] Sanchez Cuartielles, J. P., Colombo, C., Vasile, M., & Radice G., Multi-criteria comparison among several mitigation strategies for dangerous near earth objects, Journal of Guidance, Control and Dynamics, 32, 121-42, 2009. [9] Tedeschi, W.J., Remo, J.L., Schulze, J.F., Young, R.P., Experimental hypervelocity impact effects on simulated planetesimal materials, International Journal of Impact Engineering, Volume 17, Issues 4-6, 837-848, 1995 [10] NASA, Near-Earth Object Survey and Deflection Analysis of Alternatives, Report to congress, 2007. [11] Glasstone, S., The Effects of Nuclear Weapons, U.S. Atomic Energy Commission, 1962. [12] Hammerling, P., & Remo, J., NEO Interaction with Nuclear Radiation, Acta Astonautica, Vol. 36, No 6, 337-347, 1995. [13] Vasile, M., & Colombo, C., Optimal Impact Strategies for Asteroid Deflection , Journal of Guidance, Control and Dynamics, Vol. 31, No 4, 858-873, 2008. [14] Vasile, M., & Maddock, C., Design of a formation of solar pumped lasers for asteroid deflection, Advances in Space Research , Vol. 50, Issue 7, 891-905, 2012 [15] Hu, W., Scheeres, D J, Spacecraft Motion About Slowly Rotating Asteroids, Journal of Guidance, Control and Dynamics, Vol 25, pp 765-775, No 4, July-August, 2002 [16] Rossi, A., Marzari, F., Farinella, P., Orbital Evolution Around Irregular Bodies, Earth, Planets, Space, 1999, Vol 51, pp

1173-1180 [17] Schaub, H., Junkins, J., L., Analytical mechanics of space systems, AIAA Education Series, Virginia, U.,S.,A., 2003 [18] Judd, K. L., Maliar, L., Maliar, S., & Valero, R. (2014). Smolyak method for solving dynamic economic models: Lagrange interpolation, anisotropic grid and adaptive domain. Journal of Economic Dynamics and Control, 44, 92-123. [19] Broucke, R. A., & Cefola, P. J. (1972). On the equinoctial orbit elements. Celestial Mechanics, 5(3), 303-310.